Magnon crystallization in the kagomé lattice antiferromagnet

Jürgen Schnack,[1,*] Jörg Schulenburg,[2] Andreas Honecker,[3] and Johannes Richter[4,5,†]

[1] *Fakultät für Physik, Universität Bielefeld, Postfach 100131, D-33501 Bielefeld, Germany*
[2] *Universitätsrechenzentrum, Universität Magdeburg, D-39016 Magdeburg, Germany*
[3] *Laboratoire de Physique Théorique et Modélisation, CNRS UMR 8089, Université de Cergy-Pontoise, F-95302 Cergy-Pontoise Cedex, France*
[4] *Institut für Physik, Universität Magdeburg, P.O. Box 4120, D-39016 Magdeburg, Germany*
[5] *Max-Planck-Institut für Physik Komplexer Systeme, Nöthnitzer Straße 38, D-01187 Dresden, Germany*

(Dated: October 24, 2019)

We present numerical evidence for the crystallization of magnons below the saturation field at non-zero temperatures for the highly frustrated spin-half kagomé Heisenberg antiferromagnet. This phenomenon can be traced back to the existence of independent localized magnons or equivalently flat-band multi-magnon states. We also present a tentative phase diagram of this transition, thus providing information for which magnetic fields and temperatures magnon crystallization can be observed experimentally. The emergence of a finite-temperature continuous transition to a magnon-crystal is expected to be generic for spin models in dimension $D > 1$ where flat-band multi-magnon ground states break translational symmetry. The universality class of this transition depends upon the underlying lattice; for the kagomé Heisenberg antiferromagnet this transition is expected to belong to the $D = 2$ three-state Potts model universality class.

Introduction.—Strongly correlated electronic spin systems may possess unusual and thus attractive properties such as magnetization curves characterized by sequences of magnetization plateaus with possible crystallization of magnons as reported for Cd-kapellasite recently [1]. This is of course a consequence of the intricate nature of their many-body eigenstates [2–5], which, however, for, e.g., Hubbard as well as Heisenberg models under special circumstances can express itself as destructive interference that "can lead to a disorder-free localization of particles" [6]. For translationally invariant systems this automatically yields flat bands in the single-particle energy spectrum, i.e., in one-magnon space in the case of spin Hamiltonians [7–14]. Today, flat-band physics is investigated in several areas of physics, and many interesting phenomena that are related to flat bands have been found, see, e.g., Refs. [15–20]. Flat-band systems can be created using, e.g., cold atoms in optical lattices [21, 22] or by employing photonic lattices [23–25].

Among the flat-band systems, the highly frustrated quantum antiferromagnets (AFMs) play a particular role as possible solid-state realizations. There is a large variety of one-, two-, and three-dimensional lattices, where at high magnetic fields the lowest band of one-magnon excitations above the ferromagnetic vacuum is completely flat [26, 27]. These flat-band antiferromagnets exhibit several exotic features near saturation, such as a macroscopic magnetization jump at the saturation field [10], a magnetic-field driven spin-Peierls instability [28], a finite residual entropy at the saturation field [13, 14, 29], a very strong magnetocaloric effect [14, 26, 30], and an additional low-temperature maximum of the specific heat signaling the appearance of an additional low-energy scale [26].

The focus of the present paper is on a prominent example of a flat-band spin system, the spin-half kagomé Heisenberg antiferromagnet (KHAF), that is a celebrated paradigm of highly frustrated quantum magnetism [2–5]. The corresponding Hamiltonian is given by

$$\underset{\sim}{H} = J \sum_{\{i<j\}} \vec{\underset{\sim}{s}}_i \cdot \vec{\underset{\sim}{s}}_j + g\mu_B B \sum_i \underset{\sim}{s}_i^z \ , J > 0 \ , \quad (1)$$

where the first term models the Heisenberg exchange between spins at nearest neighbor sites i and j and the second term provides the Zeeman splitting in an external magnetic field.

In addition to the widely debated character of the spin-liquid ground state, the intriguing magnetization process of the KHAF has attracted much attention [1, 10, 13, 14, 26, 28, 29, 31–38]. The magnetization

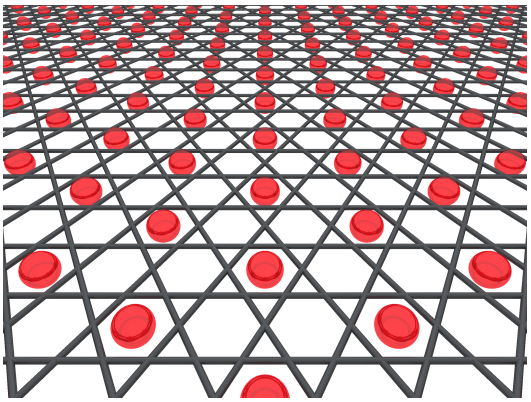

Figure 1. Sketch of a magnon crystal of localized magnons (of minimal size) on the kagomé lattice antiferromagnet. These localized magnons (red discs) are superpositions of spin flips of spins residing at the vertices of the confining basic hexagons of the kagomé lattice.

exhibits plateaus at certain fractions of the saturation magnetization, namely at $\mathcal{M}/\mathcal{M}_{\rm sat} = 3/9 = 1/3$, $5/9$, $7/9$ and likely also at $\mathcal{M}/\mathcal{M}_{\rm sat} = 1/9$ [34, 35]. In contrast to the semiclassical $\mathcal{M}/\mathcal{M}_{\rm sat} = 1/3$ plateau in the triangular-lattice Heisenberg antiferromagnet, see, e.g., [39–41], the kagomé plateau states are quantum valence-bond states [13, 14, 28, 34, 35]. Moreover, around the $\mathcal{M}/\mathcal{M}_{\rm sat} = 7/9$–plateau the flat lowest one-magnon band [10] dominates the low-temperature physics and leads to the exotic properties mentioned above. Interestingly, the $\mathcal{M}/\mathcal{M}_{\rm sat} = 7/9$ plateau state just below the jump to saturation is a magnon-crystal state that is the magnetic counterpart of the Wigner crystal state of interacting electrons in two dimensions. Since the magnon crystal spontaneously breaks translational symmetry, a finite-temperature phase transition is possible in the two-dimensional KHAF. The challenge is to find appropriate theoretical tools to describe such a transition to the magnon crystal for the quantum many-body system at hand.

Remarkably, the very existence of a flat band allows a semi-rigorous analysis of the low-temperature physics, e.g., for most of the one-dimensional flat-band quantum spin systems including the sawtooth chain [14, 29, 30] and also for a few two-dimensional systems, such as the frustrated bilayer [6, 42, 43] as well as the Tasaki lattice [44]. Such a semi-rigorous analysis builds on the existence of compact localized many-magnon states, which form either a massively degenerate GS manifold at the saturation field $B_{\rm sat}$ or a huge set of low-lying excitations for $B \lesssim B_{\rm sat}$ and $B \gtrsim B_{\rm sat}$. For the KHAF, the compact localized many-magnon states live on non-touching hexagons [10], which can be mapped to hard hexagons on a triangular lattice [13, 14, 26, 29]. This situation is depicted in Fig. 1.

On the experimental side the growing number of kagomé compounds is promising with respect to possible solid-state realizations of the kagomé flat-band physics [45–53]. Very recently the magnetization process in high field was reported for Cd-kapellasite [1]. The authors interpret the observed plateau states "as crystallizations of emergent magnons localized on the hexagon of the kagomé lattice". We will address the relation to our investigations in the discussion below.

Reliable predictions of the magnetic field–temperature regions where the magnon-crystal phase exists are useful to stimulate specific experiments. However, the semi-rigorous analysis of the flat-band properties of the KHAF based on compact localized many-magnon states, i.e., the hard-hexagon approximation (HHA) is limited because of the existence of a macroscopic number of additional *non-compact* localized many-magnon states [27]. Moreover, at non-zero temperature also non-localized eigenstates enter the game and may influence the thermodynamics of the KHAF. Thus, one may expect corrections to the theory [13, 14] taking into account only compact states.

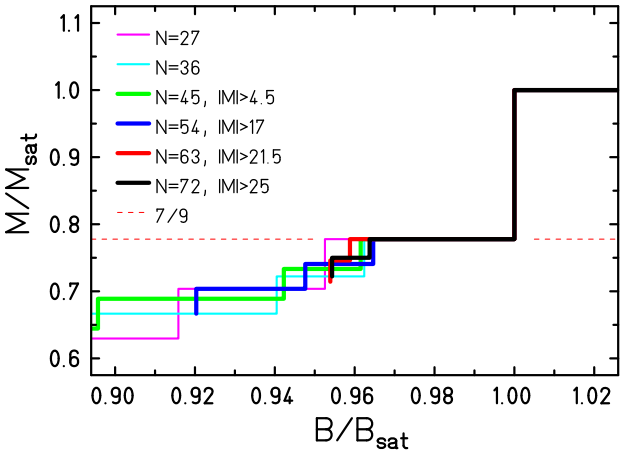

Figure 2. Magnetization $\mathcal{M}/\mathcal{M}_{\rm sat}$: Region of the 7/9 plateau for various finite size realizations of the KHAF.

Method.—To investigate the KHAF near the saturation field we present large-scale finite-temperature Lanczos (FTL) studies for finite lattices of $N = 27, 36, 45, 54, 63, 72$ sites, where we have selected only lattices exhibiting the magnon-crystal plateau at $\mathcal{M}/\mathcal{M}_{\rm sat} = 7/9$. (Note, $N = 42$ discussed in Ref. [37] is not appropriate for the current purpose, because those states giving rise to the plateau do not exist.) FTL is an unbiased numerical approach by which thermodynamic quantities are very accurately approximated by means of trace estimators [54–58]. It takes into account the full Hilbert space (in a coarse-grained way) and thus redresses the shortcomings of the HHA. Moreover, the consideration of six different lattices up to $N = 72$ allows to estimate finite-size effects.

The eigenstates of the model are characterized by the magnetic quantum number M belonging to the z-component $\underset{\sim}{S}^z$ of the total spin and the $\vec{k}$-vector of the translational symmetry. While for $N = 27$ and $N = 36$ we can take into account all sectors of $|M|$, for $N > 36$ we are restricted to sectors of larger $|M|$: $|M| > 9/2$ for $N = 45$, $|M| > 17$ for $N = 54$, $|M| > 43/2$ for $N = 63$, and $|M| > 26$ for $N = 72$, respectively. This restriction is not severe, since close to the saturation field the eigenstates with small $|M|$ become excited states with higher energy. Nevertheless, for $N > 36$ we are restricted to low enough temperatures to avoid substantial contributions of states with small $|M|$ to the partition function.

The kagomé lattices of $N = 27, 36, 45, 54, 63, 72$ sites correspond to hard-hexagon finite triangular lattices of $N_{\rm trian} = 9, 12, 15, 18, 21, 24$ sites, respectively. On symmetry grounds, triangular lattices of $N_{\rm trian} = 9, 12, 21$ sites seem to be most appropriate for our investigation [59].

Results.—First we have a look at the magnetization curve around the 7/9–plateau and the jump to saturation, see Fig. 2. The size-independence of the height of

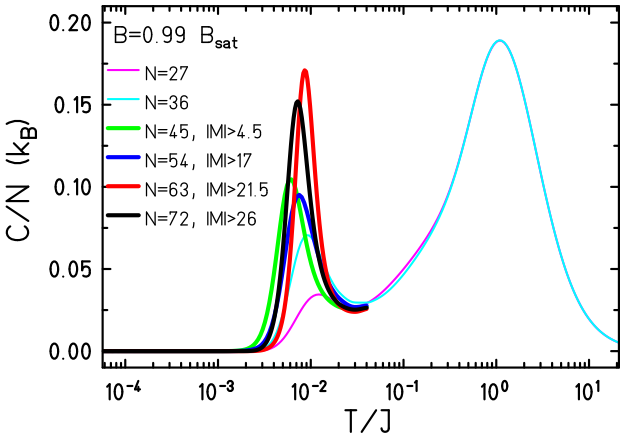

Figure 3. Specific heat for $B = 0.99B_{\rm sat}$ for various finite-size realizations of the KHAF. For $N = 45, 54, 63, 72$, where too large Hilbert subspaces had to be neglected, only the low-temperature part of the specific heat is displayed; it is virtually correct for all system sizes.

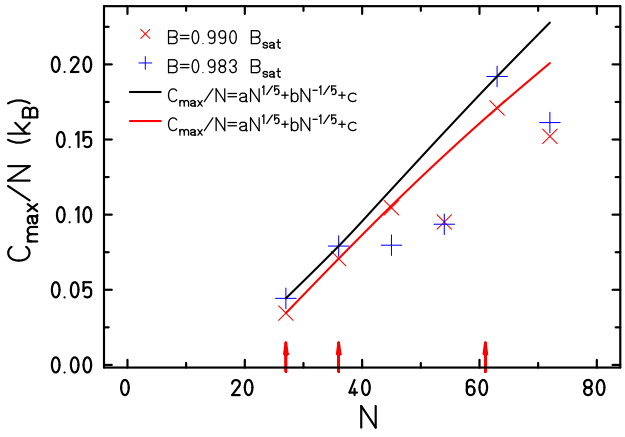

Figure 4. Maximum of the specific heat for two magnetic fields of the plateau region at the respective magnon crystallization temperature, compare Fig. 3. The solid curves according to [62] are fits to data for those sizes that correspond to highly symmetric lattices (marked by arrows) with $a = 1.34005$, $b = 4.10176$, $c = -4.66802$ for $B = 0.983B_{\rm sat}$ and $a = 0.940541$, $b = 2.471$, $c = -3.06195$ for $B = 0.990B_{\rm sat}$.

the jump is obvious. The width of the plateau, i.e., the field region where the magnon-crystal phase can exist, is about 4% of the saturation field and its finite-size dependence is weak, cf. Ref. [35].

The finite-temperature transition to the magnon-crystal phase can be driven either by temperature when fixing B in the plateau region or by the magnetic field when fixing T below the critical temperature T_c. The transition is expected to belong to the universality class of the classical two-dimensional Potts model [13, 14], one indication being that the ground states coincide with those of the HHA. This means that the transition is characterized by a power-law singularity in the specific heat C (critical exponent $\alpha = 1/3$), see, e.g., [60, 61]. Thus $C(B, T)$ is an appropriate quantity to detect the transition. For finite lattices the specific heat will not exhibit a true singularity, rather we may expect a well-pronounced peak in C that indicates the critical point. Furthermore, the peak has to become sharper with increasing N.

First we study the temperature profile $C(T)$ for two magnetic fields slightly below saturation, $B = 0.990B_{\rm sat}$ (see Fig. 3) and $B = 0.983B_{\rm sat}$ (not shown), where we present data for $N = 27, 36, 45, 54, 63, 72$. While the influence of N on the peak position $T_{\rm max}$ is rather weak, the increase of the height $C_{\rm max}$ with growing N is significant and the peaks are sharpest for $N = 63$ and $N = 72$.

Figure 4 shows the size dependence of $C_{\rm max}$ for both fields. However, we find that the increase of $C_{\rm max}$ is non-monotonic; e.g., $C_{\rm max}$ is larger for $N = 63$ than for $N = 72$. This might be attributed to geometric details of the finite lattices. The overall scaling of the height of the peak with N is in accordance with a possible phase transition to a magnon crystal, i.e., it could be expected that the height becomes a singularity for $N \to \infty$, cf. Fig. 8 in [14].

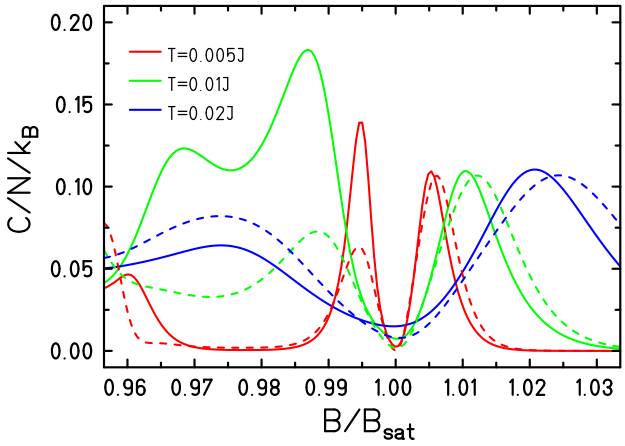

Figure 5. Specific heat vs. B at various low temperatures for the KHAF with $N = 63$ (solid curves) and $N = 36$ (dashed curves, same color for same temperature).

For the two-dimensional three-state Potts model, that we consider to be in the same universality class, the asymptotic behavior of $C_{\rm max}/N$ for large N is given by $C_{\rm max}/N \propto N^{(\alpha/2\nu)}$[62] with critical indices $\alpha = 1/3$ and $\nu = 5/6$ [60, 61]. For small N substantial corrections are to be expected [62]; corresponding scaling curves, fitted to data points that are related to highly symmetric triangular lattices, are displayed in Fig. 4.

Next we consider the field dependence of the specific heat at low temperatures $T/J = 0.005, 0.01, 0.02$, see Fig. 5, where we present data for $N = 36$ (dashed) and $N = 63$ (solid curves). A corresponding figure based on the HHA is given as Fig. 8 in [14]. There are two peaks left and right of the minimum in $C(B)$ at $B = B_{\rm sat}$ which are related to the huge set of low-lying excitations

(flat-band states in form of localized magnon states), cf. [26, 27]. The peaks are sharp at very low $T/J = 0.005$ and become broader with increasing T. The height of the maximum above $B_{\rm sat}$ is almost identical for $N = 36$ and $N = 63$; it does not correspond to a phase transition [26, 27]. However, in agreement with Fig. 3, for $T/J = 0.005$ and 0.01 the height of the maximum below $B_{\rm sat}$ is much larger for $N = 63$, while the position of this maximum is almost identical.

As already argued above, the size dependence of the maximum for $B \lesssim B_{\rm sat}$ is in accordance with a possible phase transition. It is also obvious from Fig. 5 that already at $T/J = 0.02$ the relevant maximum is very broad and the size dependence is changed, i.e., a possible critical temperature is below this T value.

A more detailed comparison of our FTL data shown in Fig. 5 with the corresponding HHA data shown as Fig. 8 of [14] provides some insight in the limitations of the HHA. The $C(B)$ plot in Fig. 8 of [14] for $T = 0.05J$ exhibits a singularity at $B \sim 0.92B_{\rm sat}$. This means that within the HHA (i) the magnon-crystal phase appears at magnetic fields significantly outside (below) the $M = 7/9$ plateau and (ii) the transition temperature is drastically overestimated.

To derive a tentative phase diagram we have calculated $C(T)$ for a fine net of B values in the plateau region, see Fig. 6(a), where we show the position $T_{\rm max}$ of the low-T peak of $C(T)$ vs B for $N = 63$ and $N = 72$. We also show the HHA result $T_c = 0.928(1 - B/B_{\rm sat})$ (straight black line) [14]. First we notice that very close to the saturation field ($0.995B_{\rm sat} \lessapprox B \leq B_{\rm sat}$) the HHA agrees well with our data. When further decreasing the magnetic field, our data for $T_{\rm max}$ deviate significantly from the HHA and $T_{\rm max}$ exhibits a maximum at about $B = 0.975B_{\rm sat}$, i.e., near the midpoint of the plateau. When approaching the lower endpoint $B_{\rm end}$ of the plateau (depicted by the vertical lines in Fig. 6) $T_{\rm max}$ decreases and we may expect that it vanishes near $B_{\rm end}$, where the magnon-crystal ground state disappears. For finite systems, as approaching $B_{\rm end}$ the relevant peak in $C(T)$ merges with low-T finite-size peaks appearing just below $B_{\rm end}$, this way masking the true behavior expected for $N \to \infty$.

We mention that the general shape of the transition curve in Fig. 6(a) resembles the phase diagram of the magnon crystallization of the fully frustrated bilayer AFM [6, 42, 43]. Therefore, we may argue that the shape of this curve is generic for two-dimensional spin models possessing flat-band multi-magnon ground states.

The height of the maximum $C_{\rm max}$ of $C(T)$ (supposed to become a power-law singularity for $N \to \infty$) is shown in Fig. 6(b) vs B for $N = 63$ and $N = 72$. The shape of these curves is dome-like with a maximum near the midpoint of the plateau. The unusual behavior at $B = B_{\rm sat}$ is discussed in Ref. [26]).

Discussion.—We may conclude that our FTL data confirm the very existence of a low-temperature magnon-crystal phase just below the saturation field as conjectured by the HHA [13, 14]. However, the B–T region where this phase exists is not properly described by the HHA.

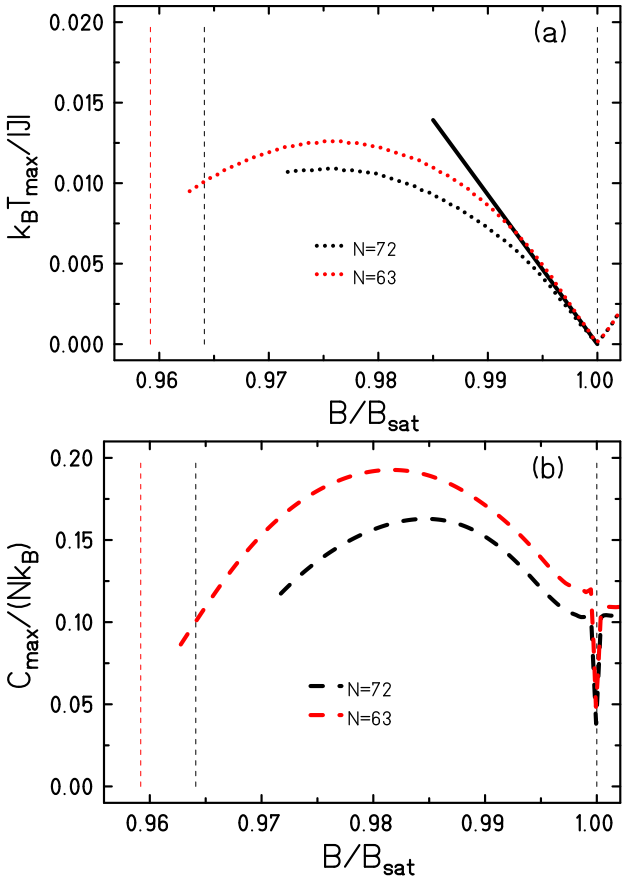

Figure 6. Phase diagram: (a) Position $T_{\rm max}$ and (b) height $C_{\rm max}$ of the low-T maximum (cf. Fig. 3) in dependence on B for $N = 63$ and $N = 72$ for fields where the maximum can be unambiguously detected. The vertical dashed lines mark the repective edges of the magnetization plateau.

Coming back to the "magnon crystallization" reported in the experimental paper [1]: Here the authors interpret the observed plateau states "as crystallizations of emergent magnons localized on the hexagon of the kagomé lattice". This concept coincides with the present study for the 7/9–plateau, but may differ for plateaus at smaller magnetization, e.g., at 1/3 and 5/9. Although these lower plateaus can be understood as magnon crystals formed at $T = 0$, it still has to be investigated whether the physical behavior for $T > 0$ differs from the scenario discussed in our paper, since the huge set of flat-band multi-magnon states determining the low-T thermodynamics near $B_{\rm sat}$ is missing for these plateaus.

This work was supported by the Deutsche Forschungsgemeinschaft (DFG SCHN 615/23-1). Computing time at the Leibniz Center in Garching is gratefully acknowledged. The authors are indebted to O. Derzhko and

J. Strečka for valuable discussions.

* jschnack@uni-bielefeld.de
† Johannes.Richter@physik.uni-magdeburg.de

[1] R. Okuma, D. Nakamura, T. Okubo, A. Miyake, A. Matsuo, K. Kindo, M. Tokunaga, N. Kawashima, S. Takeyama, and Z. Hiroi, "A series of magnon crystals appearing under ultrahigh magnetic fields in a kagomé antiferromagnet," Nat. Commun. **10**, 1229 (2019).
[2] Leon Balents, "Spin liquids in frustrated magnets," Nature **464**, 199 (2010).
[3] Oleg A. Starykh, "Unusual ordered phases of highly frustrated magnets: a review," Rep. Prog. Phys. **78**, 052502 (2015).
[4] Philippe Mendels and Fabrice Bert, "Quantum kagome frustrated antiferromagnets: One route to quantum spin liquids," Comptes Rendus Physique **17**, 455 – 470 (2016).
[5] Lucile Savary and Leon Balents, "Quantum spin liquids," Rep. Prog. Phys. **80**, 016502 (2017).
[6] Johannes Richter, Olesia Krupnitska, Vasyl Baliha, Taras Krokhmalskii, and Oleg Derzhko, "Thermodynamic properties of $Ba_2CoSi_2O_6Cl_2$ in a strong magnetic field: Realization of flat-band physics in a highly frustrated quantum magnet," Phys. Rev. B **97**, 024405 (2018).
[7] Andreas Mielke, "Ferromagnetic ground states for the Hubbard model on line graphs," J. Phys. A: Math. Gen. **24**, L73–L77 (1991).
[8] Hal Tasaki, "Ferromagnetism in the Hubbard models with degenerate single-electron ground states," Phys. Rev. Lett. **69**, 1608–1611 (1992).
[9] Jürgen Schnack, Heinz-Jürgen Schmidt, Johannes Richter, and Jörg Schulenburg, "Independent magnon states on magnetic polytopes," Eur. Phys. J. B **24**, 475 (2001).
[10] Jörg Schulenburg, Andreas Honecker, Jürgen Schnack, Johannes Richter, and Heinz-Jürgen Schmidt, "Macroscopic magnetization jumps due to independent magnons in frustrated quantum spin lattices," Phys. Rev. Lett. **88**, 167207 (2002).
[11] S. A. Blundell and M. D. Núñez-Regueiro, "Quantum topological excitations: from the sawtooth lattice to the Heisenberg chain," Eur. Phys. J. B **31**, 453–456 (2003).
[12] Johannes Richter, Jörg Schulenburg, Andreas Honecker, Jürgen Schnack, and Heinz-Jürgen Schmidt, "Exact eigenstates and macroscopic magnetization jumps in strongly frustrated spin lattices," J. Phys.: Condens. Matter **16**, S779 (2004).
[13] M. E. Zhitomirsky and Hirokazu Tsunetsugu, "Exact low-temperature behavior of a kagomé antiferromagnet at high fields," Phys. Rev. B **70**, 100403 (2004).
[14] M. E. Zhitomirsky and Hirokazu Tsunetsugu, "High field properties of geometrically frustrated magnets," Prog. Theor. Phys. Suppl. **160**, 361–382 (2005).
[15] Sebastian D. Huber and Ehud Altman, "Bose condensation in flat bands," Phys. Rev. B **82**, 184502 (2010).
[16] Siddharth A. Parameswaran, Rahul Roy, and Shivaji L. Sondhi, "Fractional quantum Hall physics in topological flat bands," Comptes Rendus Physique **14**, 816 – 839 (2013).
[17] E. J. Bergholtz and Z. Liu, "Toplogical flat band models and fractional Chern insulators," Int. J. Mod. Phys. B **27**, 1330017 (2013).
[18] Daniel Leykam, Sergej Flach, Omri Bahat-Treidel, and Anton S. Desyatnikov, "Flat band states: Disorder and nonlinearity," Phys. Rev. B **88**, 224203 (2013).
[19] Oleg Derzhko, Johannes Richter, and Mykola Maksymenko, "Strongly correlated flat-band systems: The route from Heisenberg spins to Hubbard electrons," Int. J. Mod. Phys. B **29**, 1530007 (2015).
[20] Daniel Leykam, Alexei Andreanov, and Sergej Flach, "Artificial flat band systems: from lattice models to experiments," Advances in Physics: X **3**, 1473052 (2018).
[21] Gyu-Boong Jo, Jennie Guzman, Claire K. Thomas, Pavan Hosur, Ashvin Vishwanath, and Dan M. Stamper-Kurn, "Ultracold atoms in a tunable optical kagome lattice," Phys. Rev. Lett. **108**, 045305 (2012).
[22] J. Struck, C. Ölschläger, M. Weinberg, P. Hauke, J. Simonet, A. Eckardt, M. Lewenstein, K. Sengstock, and P. Windpassinger, "Tunable gauge potential for neutral and spinless particles in driven optical lattices," Phys. Rev. Lett. **108**, 225304 (2012).
[23] Rodrigo A. Vicencio, Camilo Cantillano, Luis Morales-Inostroza, Bastián Real, Cristian Mejía-Cortés, Steffen Weimann, Alexander Szameit, and Mario I. Molina, "Observation of localized states in Lieb photonic lattices," Phys. Rev. Lett. **114**, 245503 (2015).
[24] Sebabrata Mukherjee, Alexander Spracklen, Debaditya Choudhury, Nathan Goldman, Patrik Öhberg, Erika Andersson, and Robert R. Thomson, "Observation of a localized flat-band state in a photonic Lieb lattice," Phys. Rev. Lett. **114**, 245504 (2015).
[25] F. Baboux, L. Ge, T. Jacqmin, M. Biondi, E. Galopin, A. Lemaître, L. Le Gratiet, I. Sagnes, S. Schmidt, H. E. Türeci, A. Amo, and J. Bloch, "Bosonic condensation and disorder-induced localization in a flat band," Phys. Rev. Lett. **116**, 066402 (2016).
[26] Oleg Derzhko and Johannes Richter, "Universal low-temperature behavior of frustrated quantum antiferromagnets in the vicinity of the saturation field," Eur. Phys. J. B **52**, 23–36 (2006).
[27] O. Derzhko, J. Richter, A. Honecker, and H.-J. Schmidt, "Universal properties of highly frustrated quantum magnets in strong magnetic fields," Low Temp. Phys. **33**, 745–756 (2007).
[28] Johannes Richter, Oleg Derzhko, and Jörg Schulenburg, "Magnetic-field induced spin-Peierls instability in strongly frustrated quantum spin lattices," Phys. Rev. Lett. **93**, 107206 (2004).
[29] Oleg Derzhko and Johannes Richter, "Finite low-temperature entropy of some strongly frustrated quantum spin lattices in the vicinity of the saturation field," Phys. Rev. B **70**, 104415 (2004).
[30] M. E. Zhitomirsky and Andreas Honecker, "Magnetocaloric effect in one-dimensional antiferromagnets," J. Stat. Mech.: Theor. Exp. , P07012 (2004).
[31] Kazuo Hida, "Magnetization process of the $S = 1$ and $1/2$ uniform and distorted kagome Heisenberg antiferromagnets," J. Phys. Soc. Jpn. **70**, 3673 (2001).
[32] Andreas Honecker, Jörg Schulenburg, and Johannes Richter, "Magnetization plateaus in frustrated antiferromagnetic quantum spin models," J. Phys.: Condens. Matter **16**, S749 (2004).
[33] D. C. Cabra, M. D. Grynberg, P. C. W. Holdsworth,

A. Honecker, P. Pujol, J. Richter, D. Schmalfuß, and J. Schulenburg, "Quantum kagomé antiferromagnet in a magnetic field: Low-lying nonmagnetic excitations versus valence-bond crystal order," Phys. Rev. B **71**, 144420 (2005).

[34] Satoshi Nishimoto, Naokazu Shibata, and Chisa Hotta, "Controlling frustrated liquids and solids with an applied field in a kagome Heisenberg antiferromagnet," Nat. Commun. **4**, 2287 (2013).

[35] Sylvain Capponi, Oleg Derzhko, Andreas Honecker, Andreas M. Läuchli, and Johannes Richter, "Numerical study of magnetization plateaus in the spin-$\frac{1}{2}$ kagome Heisenberg antiferromagnet," Phys. Rev. B **88**, 144416 (2013).

[36] Hiroki Nakano and Toru Sakai, "Numerical-diagonalization study of magnetization process of frustrated spin-1/2 Heisenberg antiferromagnets in two dimensions: Triangular- and kagome-lattice antiferromagnets," J. Phys. Soc. Jpn. **87**, 063706 (2018).

[37] Jürgen Schnack, Jörg Schulenburg, and Johannes Richter, "Magnetism of the $N = 42$ kagome lattice antiferromagnet," Phys. Rev. B **98**, 094423 (2018).

[38] Xi Chen, Shi-Ju Ran, Tao Liu, Cheng Peng, Yi-Zhen Huang, and Gang Su, "Thermodynamics of spin-1/2 kagome Heisenberg antiferromagnet: algebraic paramagnetic liquid and finite-temperature phase diagram," Science Bulletin **63**, 1545–1550 (2018).

[39] A. V. Chubukov and D. I. Golosov, "Quantum theory of an antiferromagnet on a triangular lattice in a magnetic field," J. Phys.: Condens. Matter **3**, 69 (1991).

[40] Andreas Honecker, "A comparative study of the magnetization process of two-dimensional antiferromagnets," J. Phys.: Condens. Matter. **11**, 4697 (1999).

[41] D. J. J. Farnell, R. Zinke, J. Schulenburg, and J. Richter, "High-order coupled cluster method study of frustrated and unfrustrated quantum magnets in external magnetic fields," J. Phys.: Condens. Matter **21**, 406002 (2009).

[42] Fabien Alet, Kedar Damle, and Sumiran Pujari, "Sign-problem-free Monte Carlo simulation of certain frustrated quantum magnets," Phys. Rev. Lett. **117**, 197203 (2016).

[43] Oleg Derzhko, Taras Krokhmalskii, and Johannes Richter, "Emergent Ising degrees of freedom in frustrated two-leg ladder and bilayer $s = \frac{1}{2}$ Heisenberg antiferromagnets," Phys. Rev. B **82**, 214412 (2010).

[44] M. Maksymenko, A. Honecker, R. Moessner, J. Richter, and O. Derzhko, "Flat-band ferromagnetism as a Pauli-correlated percolation problem," Phys. Rev. Lett. **109**, 096404 (2012).

[45] J. L. Atwood, "Kagome lattice - a molecular toolkit for magnetism," Nat. Mater. **1**, 91–92 (2002).

[46] P. Mendels, F. Bert, M. A. de Vries, A. Olariu, A. Harrison, F. Duc, J. C. Trombe, J. S. Lord, A. Amato, and C. Baines, "Quantum magnetism in the paratacamite family: Towards an ideal kagomé lattice," Phys. Rev. Lett. **98**, 077204 (2007).

[47] F. Bert, S. Nakamae, F. Ladieu, D. L'Hôte, P. Bonville, F. Duc, J.-C. Trombe, and P. Mendels, "Low temperature magnetization of the $S = \frac{1}{2}$ kagome antiferromagnet $ZnCu_3(OH)_6Cl_2$," Phys. Rev. B **76**, 132411 (2007).

[48] Yoshihiko Okamoto, Masashi Tokunaga, Hiroyuki Yoshida, Akira Matsuo, Koichi Kindo, and Zenji Hiroi, "Magnetization plateaus of the spin-$\frac{1}{2}$ kagome antiferromagnets volborthite and vesignieite," Phys. Rev. B **83**, 180407 (2011).

[49] T.-H. Han, J. S. Helton, S. Chu, D. G. Nocera, J. A. Rodriguez-Rivera, C. Broholm, and Y. S. Lee, "Fractionalized excitations in the spin-liquid state of a kagome-lattice antiferromagnet," Nature **492**, 406–410 (2012).

[50] Kazuya Katayama, Nobuyuki Kurita, and Hidekazu Tanaka, "Quantum phase transition between disordered and ordered states in the spin-$\frac{1}{2}$ kagome lattice antiferromagnet $(Rb_{1-x}Cs_x)_2Cu_3SnF_{12}$," Phys. Rev. B **91**, 214429 (2015).

[51] H. Ishikawa, M. Yoshida, K. Nawa, M. Jeong, S. Krämer, M. Horvatić, C. Berthier, M. Takigawa, M. Akaki, A. Miyake, M. Tokunaga, K. Kindo, J. Yamaura, Y. Okamoto, and Z. Hiroi, "One-third magnetization plateau with a preceding novel phase in volborthite," Phys. Rev. Lett. **114**, 227202 (2015).

[52] M. R. Norman, "Colloquium: Herbertsmithite and the search for the quantum spin liquid," Rev. Mod. Phys. **88**, 041002 (2016).

[53] M. Yoshida, K. Nawa, H. Ishikawa, M. Takigawa, M. Jeong, S. Krämer, M. Horvatić, C. Berthier, K. Matsui, T. Goto, S. Kimura, T. Sasaki, J. Yamaura, H. Yoshida, Y. Okamoto, and Z. Hiroi, "Spin dynamics in the high-field phases of volborthite," Phys. Rev. B **96**, 180413 (2017).

[54] J. Jaklič and P. Prelovšek, "Lanczos method for the calculation of finite-temperature quantities in correlated systems," Phys. Rev. B **49**, 5065–5068 (1994).

[55] Jürgen Schnack and Oliver Wendland, "Properties of highly frustrated magnetic molecules studied by the finite-temperature Lanczos method," Eur. Phys. J. B **78**, 535–541 (2010).

[56] Oliver Hanebaum and Jürgen Schnack, "Advanced finite-temperature Lanczos method for anisotropic spin systems," Eur. Phys. J. B **87**, 194 (2014).

[57] Burkhard Schmidt and Peter Thalmeier, "Frustrated two dimensional quantum magnets," Phys. Rep. **703**, 1–59 (2017).

[58] Eva Pavarini, Erik Koch, Richard Scalettar, and Richard M. Martin, eds., "The physics of correlated insulators, metals, and superconductors," (2017) Chap. The Finite Temperature Lanczos Method and its Applications by P. Prelovšek, ISBN 978-3-95806-224-5.

[59] B. Bernu, C. Lhuillier, and L. Pierre, "Signature of Néel order in exact spectra of quantum antiferromagnets on finite lattices," Phys. Rev. Lett. **69**, 2590 (1992).

[60] F. Y. Wu, "The Potts model," Rev. Mod. Phys. **54**, 235–268 (1982).

[61] T. Nagai, Y. Okamoto, and W. Janke, "Crossover scaling in the two-dimensional three-state Potts model," Condens. Matter Phys. **16**, 23605 (2013).

[62] Jae-Kwon Kim and D. P. Landau, "Corrections to finite-size-scaling in two dimensional Potts models," Physica A **250**, 362–372 (1998).